J. Cosmet. Sci., 64, 243–260 (July/August 2013)

Influence of various environmental parameters on sweat gland activity

ROGER L. MCMULLEN, TIM GILLECE, GUOJIN LU, DONNA LAURA, and SUSAN CHEN *Department of Materials Science, Corporate R&D, Ashland Specialty Ingredients, Wayne, NJ.*

Accepted for publication January 31, 2013.

Synopsis

The choice of environmental conditions when conducting antiperspirant studies greatly affects the quantity of sweat output. Our initial goal in this work was to develop an in-house procedure to test the efficacy of antiperspirant products using replica techniques in combination with image analysis. To ameliorate the skin replica method, we conducted rheological studies using dynamic mechanical analysis of the replica formulation. In terms of sweat output quantification, our preliminary results revealed a considerable amount of variation using the replica technique, leading us to conduct more fundamental studies of the factors that influence sweating behavior and how to best design the experimental strategy. In accordance with the FDA's protocol for antiperspirant testing, we carried out gravimetric analyses of axillae sweating under a variety of environmental conditions including temperature and humidity control. Subjects were first acclimatized in an environmentally controlled room for 30 min, and then placed in a sauna for an additional 30 or 45 min, depending on which test we administered. In Test 1 (30 min total in the sauna), the first 10 min in the sauna was another equilibration period, followed by a 20 min sweat production stage. We monitored axillae sweating during the last 20 min in the sauna by gravimetric analysis. At time (t) = 30 min in the sauna, skin replicas were taken and later analyzed using imaging and image analysis techniques. Test 1 was carried out on over 25 subjects, both male and female, from various racial backgrounds. In Test 2, subjects spent 45 min in the sauna after the initial 30-min period in the environmental room. During the 45 min, we obtained gravimetric readings of absorbent pads placed in the axillae. We conducted studies at various temperature and relative humidity settings. We also studied the influence of several external parameters on sudoriferous activity. Test 2 was a range-finding experiment on two subjects to determine the optimized environmental conditions for the hot room procedure. In addition to the replica and gravimetric techniques, we also measured flux density to determine the onset of firing of sweat glands to ensure that our environmental preconditioning step (30 min in the environmental room) brought subjects to the point that their sweat glands were activated. Although flux density measurements are usually carried out to determine transepidermal water loss (TEWL), we found that they can be equally useful for monitoring the onset of sweat production. Thermal infrared imaging experiments were also carried out allowing us to generate full-body images of subjects containing anatomical thermal distribution data with high accuracy. Overall, we conclude that our in-house hot room procedure offers much potential as an effective and cost-efficient screening tool for narrowing copious antiperspirant formulations to a select few for expensive clinical evaluation.

Address all correspondence to Roger McMullen at rmcmullen@ashland.com.

INTRODUCTION

In *Homo sapiens*, the principal mode of thermoregulation is accomplished by evaporative cooling that takes place when sweat is secreted from eccrine glands and evaporated from the surface of the skin. Overall, such a process ensures that the body's core temperature does not significantly rise above 37°C to levels that can lead to heat exhaustion or hyperthermia. There are about 2–5 million eccrine glands distributed over the surface of the body, which carry out this function (1). In addition, there are approximately 100,000 apocrine glands localized in specific regions of the body, most notably the axillae. Although apocrine glands secrete substances that eventually break down to malodorous compounds, antiperspirant treatments target eccrine glands that are located in the axillae. Therefore, understanding how various external and internal stimuli affect eccrine sweating is of great concern for those involved in antiperspirant technology (2).

In addition to thermoregulation, sweating also occurs due to emotional/mental stimulation as well as during gustation. In recent years, Wilke *et al*. provided an updated review covering most aspects of these phenomena (3). We often associate emotional sweating with profuse sweating that occurs in the palms, soles, or axillae (4). Most researchers believe that sweating in these locations during stressful events has evolutionary origins that allowed us to reduce the surface friction of the otherwise high-friction zones of the palms or soles (5). Likewise, secretion of eccrine and apocrine sweat from the axillae during distress would facilitate pheromone signaling to other members of our species. Gustatory sweating occurs in many individuals during digestion and is particularly evident during the consumption of spicy food. Such sweating is normally confined to the face, forehead, scalp, and neck (3).

Thermoregulatory sweating is affected by many internal and external factors including climatic conditions, diet, physical/mental state, and body posture. The most evident climatic factors include temperature, humidity, and dewpoint. At high humidity and dewpoint, cooling is less efficient (6,7). Diet and fluid intake also play a major role in determining sweating behavior. Not surprisingly, many studies were carried out by military agencies during the 1940s to understand how man could better survive the harsh elements, such as conditions found in the desert (8). Furthermore, it may come as no surprise that clothing is also a critical factor of perspiration. Physical stamina and fitness form the basis of sweat capacity, and more fit individuals are likely to be more efficient sweaters (9). Likewise, the sweat gland apparatus is less active in the elderly, usually beginning around the sixth decade (10,11). Therefore, less fit and older individuals will tend to overheat much easier. Finally, posture also governs sweating. Whether we are sitting or standing, or even crossing our legs, will influence our sweating behavior (7). Posture becomes increasingly important during antiperspirant testing when subjects are placed in climate-controlled environments for prescribed periods. In addition, the pH of axillary skin surface fluctuates depending on the time of day (12). This can have profound implications on the efficacy of antiperspirant treatments, whose mechanism of action is pH dependent. Overall, all of these factors must be considered when monitoring sweating behavior.

Our initial objective in this work was to develop an in-house procedure to test the efficacy of antiperspirant products using replica techniques in combination with image analysis (13). To better understand the rheological profile of the replica impression material, we used dynamic mechanical analysis (DMA) to monitor rheological parameters, such as the elastic modulus (E), loss modulus (E), and damping ability (tan δ), as a function of curing

time. These data provided us with sufficient information to establish appropriate testing parameters, ensuring that we used proper quantities and induction times in the test protocol. To understand the variability of sweat output, we carried out gravimetric measurements to monitor the kinetics of sweat uptake by absorbent pads placed in the axillae. Proper choice of equilibration times in the environmental room required that we also conduct flux measurements of water vapor diffusion, which were carried out on the inner forearm. In addition, we used thermal infrared (IR) imaging to map the temperature distribution across all surface anatomical regions. This allowed us to monitor the heating (environmentally controlled) and subsequent cooling (eccrine sweating) of various regions of the body. Based on the combined results of the gravimetric kinetic studies, flux measurements, and IR thermal imaging, we find that our choice of parameters (temperature, relative humidity (RH), and acclimatization times) for the skin replica studies is valid.

MATERIALS AND METHODS

Sweat gland activity was monitored using gravimetric analysis and skin replica techniques. We carried out gravimetric analysis to monitor sweating in the axillae. Skin replicas were obtained from the inner forearm and later analyzed using image analysis techniques—providing the quantity of active glands per unit area. Two different tests were conducted, one where the subjects spent 30 min in the sauna (Test 1) and the other 45 min (Test 2). Replicas and gravimetric analysis were carried out simultaneously in Test 1, whereas only gravimetric analysis was completed in Test 2. We used various temperature and humidity control conditions in the sauna, which are indicated in the Results and Discussion section. Unless otherwise indicated, the subjects were acclimatized in an environmental room prior to entry into the sauna—for both Tests 1 and 2. In addition, we carried out DMA studies of the replica formulation to ensure proper mixing and curing kinetics. Flux density measurements were used to corroborate the chosen acclimatization schedule. Thermal imaging allowed for the determination of the anatomical temperature distribution in the subjects as a function of time and the selected environment.

QUANTIFICATION OF SUDORIFEROUS BEHAVIOR

An environmental room was constructed to house a sauna and also to serve as an acclimatization area for subjects prior to entry into the sauna. We designed the room in such a manner as to provide a serene environment allowing the subjects to experience similar comforts and sentiments as in a spa. After the installation of a ceramic floor, the entire room was painted and decorated using modern decor. The underlying walls and floor of the environmental room are constructed of concrete thereby preventing excessive temperature/humidity loss from the room and temperature/humidity invasion from the external environment. The dimensions of the environmental room are 5 m length, 2.5 m width, and 2.2 m height. The sauna, Model FRB-022LCND, was purchased from Sauna King Products, San Leandro, CA. It is an IR sauna constructed of cedar wood and has five internal heaters. The operating temperature is between 30°C and 60°C (86°F and 140°F). The humidity inside the chamber is controlled with a humidifier (Model HM5082; Holmes, Boca Raton, FL) connected to a humidity controller (Model 5200; Electro-tech Systems,

Inc., Glenside, PA). Inside the environmental room, temperature and humidity are also controlled using two floor heaters (Model HZ-519; Honeywell, Morristown, NJ) and a cool mist humidifier (Model HM3655; Holmes, Boca Raton, FL). During testing, temperature, humidity, and dewpoint were monitored every minute in the sauna, in the environmental room, outside the environmental room in the building, and outside of the building in a shaded area. These data were recorded using data loggers (Model DVTH 421-338-0023; purchased from Supco, Allenwood, NJ), and were transferred to computer by USB cable where they could be analyzed using software provided by Supco. The barometric pressure was also recorded at the beginning of all experimental sessions using an aneroid (mechanical) barometer (Model Proteus; Maximum Inc., New Bedford, MA).

Unless otherwise indicated, subjects are allowed to acclimate for 30 min in the environmental room prior to entry into the sauna. During this time, they are discouraged from engaging in stressful conversation or work-related reading. The temperature and humidity of the room are (normally) maintained constant at approximately 28°C (84°F) and 40% RH, corresponding to a dew-point temperature of roughly 14°C (57°F) and saturation vapor pressure of 3.98 kPa. All subjects were dressed in a uniform consisting of cotton slacks (Model RN85080; La Difference, Mexico) and cotton T-shirts (I2701; Fruit of the Loom, Inc., Bowling Green, KY). For safety reasons, the blood pressure and pulse rate of each subject were recorded before entry into the sauna using a blood pressure monitor kit (Model HEM-780; Omron, Kyoto, Japan). If blood pressure readings indicated any degree of hypertension, the subject was immediately dismissed from participating in the test. The following guidelines were used to determine the level of severity of hypertension: mild hypertension (systolic blood pressure = 140–160 mm Hg; diastolic blood pressure = 90–100 mm Hg), moderate hypertension (systolic blood pressure = 160–200 mm Hg, diastolic blood pressure = 100–120 mm Hg), and severe hypertension (systolic blood pressure = above 200 mm Hg, diastolic blood pressure = above 120 mm Hg). We measured resting heart rate (no physical exertion) and eliminated any subjects from the study whose monitored values were greater than 90 bpm.

Once the subject reached equilibrium in the environmental room, they entered the sauna for a total of either 30 (Test 1) or 45 min (Test 2). In Test 1, the first 10 min is an equilibrium period followed by a 20 min sweat production period. At $t = 10$ min, the subject was given two pre-weighed feminine hygiene pads (Stayfree, Ultrathin Overnight Pads with Wings; McNeil-PPC, Inc., Skillman, NJ), which they place (folded) in the left and right axillae. At $t = 30$ min, the weight of the absorbent pad is measured using an electronic balance (Scout Pro Balance, Ohaus, Pine Brook, NJ). After the pad is weighed, replica measurements are conducted. In Test 2, the subject enters the chamber and is immediately given the pads to place in the axillae. The pads are weighed every 5 min until the conclusion of the test. In Test 1, we recruited more than 25 subjects, both male and female, from diverse racial backgrounds and ranging in age from 30 to 45 years. In Test 2, two male subjects participated in a battery of range-finding experiments. Subject 1—38 years old, 62 in. height, 135 lb. weight, and of Chinese origin. Subject 2—43 years old, 70 in. height, 175 lb. weight, and American of Northern European ancestry. These two subjects had no history within the last 5 years of antiperspirant usage.

In several experiments, subjects were preconditioned using an exercise bike (Schwinn Active 10 Series; Nautilus Inc., Vancouver, WA). In other experiments, subjects were placed in a cool room (2°C and 80% RH) for the first 30 min of the test, then directly entered the sauna. Also, the influence of hot (76°C) and room temperature (22°C) water ingestion

on sweating was investigated by giving the subjects 250 ml of water at $t = 20$ min in the sauna (water was consumed within 5 min).

RHEOLOGICAL ANALYSIS AND PREPARATION OF REPLICAS

To obtain replicas of the skin-surface structure, including sweat bead topography, we used Silflo impression resin in combination with supplied thinner and catalyst (CuDerm, Dallas, TX). The preparation consisted of (i) Adding 10 drops of thinner to 4.0 g of resin, mixing thoroughly, and allowing 20 min for equilibration. (ii) Five drops of catalyst were subsequently added to the resin/thinner mixture, followed by 10 s of meticulous mixing, and ensuing application to the skin or DMA geometry. Because the resin hardens via a time-dependent, condensation curing process, where the hydroxyl-terminated silicone chains are catalyzed into a crosslinked, elastomeric network, the kinetics and rheology of the curing process were studied prior to *in vivo* testing. A DMTA Mark IV Dynamic Mechanical Analyzer (TA Instruments, New Castle, DE) was used to approximate the gel point (i.e., $E' = E''$) of the curing resin (14). Aliquots of the catalyzed resin were loaded into a compression fixture (17-mm-diameter stainless steel plates) and dynamic time sweep experiments ($\omega = 1$ Hz, $\gamma = 0.5\%$, gap = 1 mm, 25.7°C, $n = 6$) were executed to follow the changes in viscoelasticity as a function of time. To simulate the presence of a bead of sweat in contact with the curing resin, a 20 µl droplet of $\rho = 18.2$ MΩ·cm purified water (Millipore, Burlington, MA) was added to the surface of the loaded resin prior to adjusting the DMA geometry to the 1-mm testing gap and starting the test.

During the *in vivo* perspiration tests, silicone impressions were only taken during Test 1. In this particular test, we used Procedure 1 (described in the section above) in which case approximately 10 drops of thinner is added to the impression material at $t = 10$ min in the sauna. This mixture is allowed to sit until $t = 30$ min, when 5 drops of catalyst were added. The resulting mixture is thoroughly, but gently, mixed prior to application avoiding the formation of air bubbles (note that mixing was carried out in the environmentally controlled room, not the sauna). Four skin replica rings were placed on the upper part of the inner forearms of the subjects for the last 5 min they spent in the sauna. Also, the day prior to experiments, all subjects were thoroughly shaved in the inner former area so that hair fibers would not interfere with the replica measurements of sweat protrusions. Subjects did not use any type of cosmetic or pharmaceutical products on their inner forearm region for at least 1 day prior to the examination (In fact, in almost all cases, subjects reported never treating their skin with products.). Prior to the tests, the forearm of each subject was gently washed with Dove soap (Dove beauty bar; Unilever, Trumbull, CT). Image analysis methods were used in combination with skin replica analysis to quantify the number of active sweat glands per given area. This technique is largely based on a published report by Keyhani *et al.* (13). Image processing and analysis were carried out using Adobe Photoshop CS5 (Adobe Systems Inc., San Jose, CA) and ImageJ (http://rsbweb.nih.gov/ij/).

IR THERMAL IMAGING

We conducted thermal imaging measurements with a FLIR Systems camera (Model P620; FLIR Systems Inc., Wilsonville, OR). The thermal imaging camera was mounted on a tripod

at a fixed distance from the subject to obtain a full-body image. All dimensions were kept constant throughout the experiments. The image data consist of a two-dimensional image grid with temperature measurements plotted on a third axis using a color image scale.

FLUX DENSITY MEASUREMENTS

To gain insight into the impact of a subject's recent environmental history on the quality of the final 30 min acclimatization process (i.e., equilibration phase before entering the hot box), a new method was applied *in vivo* to two experienced subjects. Vapor flux measurements were performed on the two male subjects after 15 min pre-equilibration in a cool (6.3°C, 66% RH) or warm (24°C, 28% RH) environment. Flux density measurements were commenced during the final acclimatization stage (30.5°C, 36.5% RH) using an AquaFlux AF200 (Biox Systems, London, UK) evaporimeter configured with a Teflon 7 mm orifice measurement cap. The AF200 was used to examine variations in the vapor flux density as a function of equilibration time. For each subject, three zones of the middle of the left volar forearm were screened at 0, 30, and 60 min of the final acclimatization process. The device was transferred rapidly from park (idle), or from zone to zone, to reduce the impact of ambient humidity on the skin surface water loss results. The maximum time for each zone measurement was 80 s and the target precision for the evaluation of the equilibrium flux density was ≤ 0.075 $gm^{-2}h^{-1}$ standard deviations, which is calculated from the running average of 10 consecutive flux readings. Two-sample Student's *t*-tests ($\alpha = 0.10$, two-tailed), assuming equal variances, were performed on the flux density results to test the null hypotheses (H_0: $\mu_1 - \mu_2 \neq 0$) that (i) environmental pre-equilibration time and conditions have no influence on a single subject's flux density response; (ii) in addition, when compared at the same pre-equilibration time and environmental conditions, the flux density response between subjects is not statistically significant (XLSTAT, Addinsoft, NY).

RESULTS AND DISCUSSION

We used several techniques to monitor the amount of perspiration by test participants. A skin replica technique was used following a previously published procedure (13). To gain further insight into the gelation of the replica material, we carried out rheological measurements using DMA. In turn, a method similar to the FDA monograph was used to measure axillae sweating using absorbent pads (15). We also used thermal IR imaging to monitor overall skin-surface temperature and the anatomical temperature distribution. In all of these tests, subjects were first acclimated in an environmentally controlled room (27°C, 50% RH) for 30 min and then placed in a similarly controlled sauna chamber—specific temperature and humidity settings are provided in the following text. In addition, we monitored variations in flux density of water vapor diffusing through the skin barrier either in the form of TEWL and/or insensible perspiration.

RHEOLOGY OF SILFLO FORMULATION

Figure 1 shows the average ($n = 6$) curing profile of the Silflo replica formulation at ambient conditions as a function of time. The error bars express the standard deviation of

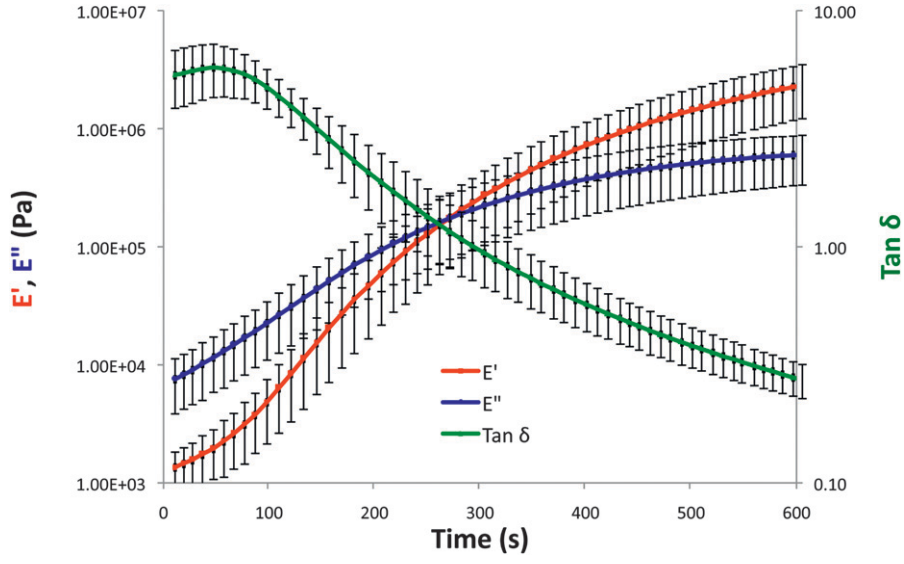

Figure 1. Average dynamic time sweep profile for curing of replicas as a function of time. The average gel point for the formulation, where E′ = E″, occurs at 297 ± 12s (n = 5; 1 Hz; 25.7°C).

E′, E″, and tan δ at each time point in the experiment. The deviation in viscoelasticity between trials reflects the inherent randomness in the logistics of crosslinking a slow-moving, highly viscous prepolymer—including slight variations in the volume of each catalyst droplet, mixing efficiency, and sample loading time. Although the resin consistency varies slightly with time from trial to trial, the mean time of E′/E″ inversion is approximately 5 min (±12 s). Hence, 5 min was chosen as the length of curing for acquiring *in vivo* impressions. In reality, however, the replicas were not removed for another 2–3 min (i.e., total cure t = 7–8 min) due to post-testing interviews. From the rheology data (Figure 1), the advantage of waiting an additional 2–3 minutes ensures a rubbery consistency and that E′>>E″ (16). In general, excess curing time (>5 min) does not influence the quality of the replica and ultimately produces a stronger, more uniform, and cohesive impression that is easily peeled from the substrate.

QUANTIFICATION OF PERSPIRATION WITH SKIN REPLICAS

After 30 min equilibration in the environmental room, subjects were placed in the sauna (usually at 45°C and 35% RH) and allowed to acclimatize for 10 min followed by a 20 min perspiration period (Test 1). At the beginning of the perspiration period, absorbent pads were placed in the axillae—they were later weighed at the end of the test. After a total of 30 min in the chamber, replicas were obtained on the volar forearm, using a four-quadrant sampling area immediately adjacent to the antecubital fossa (inner elbow). The replicas were allowed to set for 5 min, then removed. Quantification of the number of active eccrine pores was achieved using the image analysis software, ImageJ.

Figure 2 contains a photograph showing the position of the replica rings on the inner forearm. Also included is an image of a replica in which the active sweat glands produced a protrusion on the surface of the skin resulting in a negative cast on the replica. Therefore, dark large dots in the image correspond to beads of sweat. Using image analysis software, the image can be processed so that dark dots can be isolated on a white background and then counted to determine the number of active glands per unit area. A full study illustrating the effects of climatic conditions, contrast between right and left arms, gender differences, etc. was already published using this technique (13). We found similar results using this approach and, therefore, will not elaborate more on the subject for the sake of brevity.

KINETICS OF AXILLAE PERSPIRATION BEHAVIOR

We controlled and monitored several environmental parameters and their influence on sweat gland activity. Unlike the replica experiments described above, subjects spent 45 min (Test 2) in the sauna chamber during the kinetic studies. The first series of experiments involved examining the effect of temperature and humidity on perspiration output. In all experiments (except where indicated), subjects were acclimatized for 30 min at 27°C and 50% RH prior to exposure to the indicated conditions. A typical plot of perspiration vs. time is provided in Figure 3 for both the left and right axillae of one of the subjects. There are two distinct slopes that appear in all of the plots—from time 0 to 20 min, and from time 25 to 45 min. Initially, we attempted to treat the data using quantitative models and several theories of diffusion. Unfortunately, the situation governed by the absorbent pads, which adsorb sweat from the surface of skin, is not accurately depicted by simple diffusion processes. Interestingly, after the inflection point at 25 min, the plot is characterized by a second slope greater in rate. The reported perspiration rates in this study were determined from measurements of the slope from 25–45 min. Selected

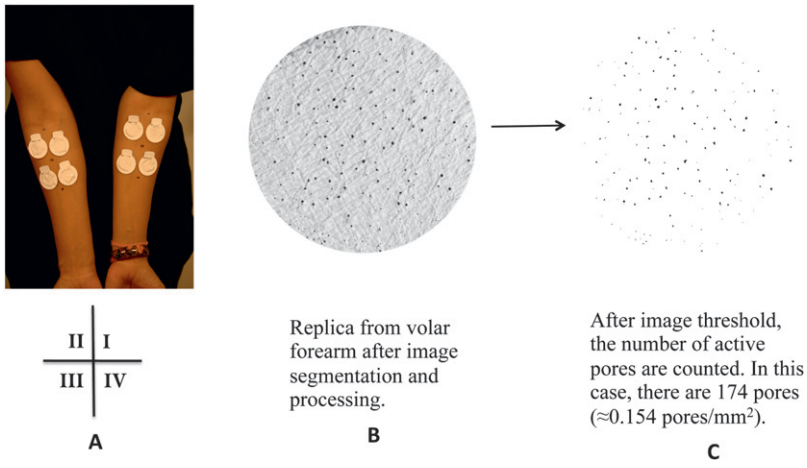

Figure 2. (A) Photograph of the volar forearms of a subject containing replica rings placed on a four quadrant layout. (B) Digital image of a cast from the volar forearm region along with (C) its image processed counterpart containing isolated sweat profusions on a white background (counted). This was the key output parameter for Test 1.

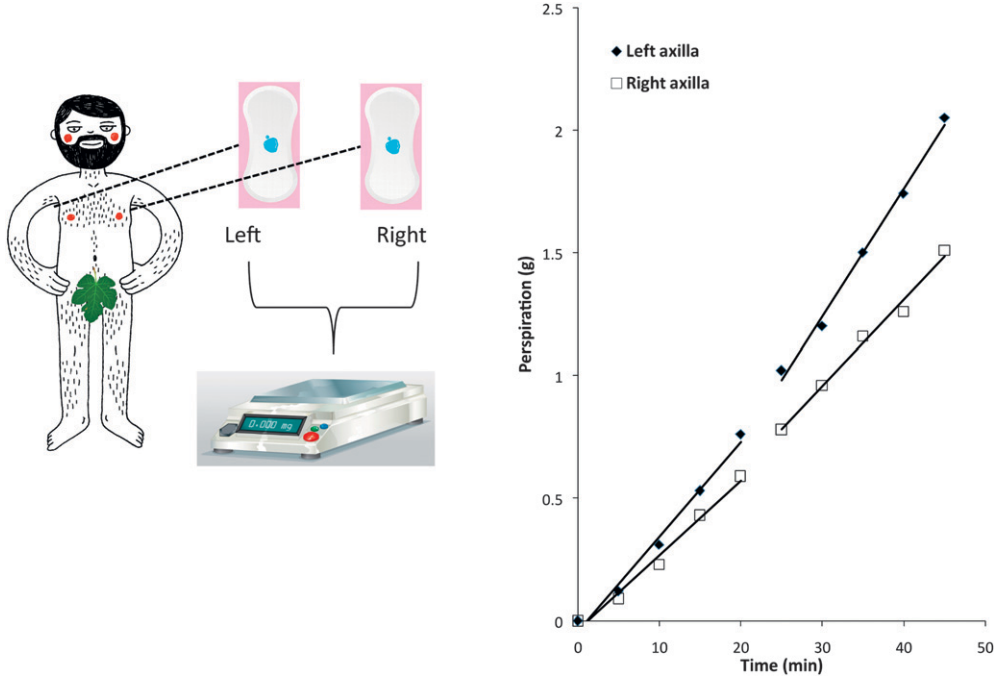

Figure 3. In Test 2, subjects were placed in the sauna chamber with absorbent pads in the axillae region, which were weighed for a period of 45 min in increments of 5 min.

data are provided in Table I to demonstrate the effects of environmental conditions on axillae sweating.

For all of the studies described in this section, two subjects were chosen to undergo a rigorous series of tests. Reported values represent an average of two measurements conducted on different days. While this may seem like a small sampling pool, we found the results to be extremely reproducible when all environmental parameters were carefully controlled. As indicated in Table I, increasing the RH increases the rate of perspiration in both subjects. Likewise, we observe a similar effect for an increase in temperature. Data are shown for 30% RH and temperatures of 37, 45, and 52°C. This humidity may be easily attained at all three temperatures. However, when we try to go to higher humidity

Table I
Perspiration Rates (g/min) Calculated from Plots of Perspiration vs. Time for Various Temperature and Humidity Settings in the Sauna Chamber

	Subject 1		Subject 2	
	Left	Right	Left	Right
30% RH, 37°C	0.0414 ± 0.006	0.0406 ± 0.003	0.0189 ± 0.006	0.0149 ± 0.004
80% RH, 37°C	0.0848 ± 0.002	0.0893 ± 0.007	0.0377 ± 0.000	0.0357 ± 0.000
30% RH, 45°C	0.0790 ± 0.001	0.0848 ± 0.005	0.0405 ± 0.002	0.0295 ± 0.002
60% RH, 45°C	0.1212 ± 0.058	0.1238 ± 0.055	0.0757 ± 0.001	0.0661 ± 0.004
30% RH, 52°C	0.1384 ± 0.009	0.1391 ± 0.007	0.1044 ± 0.006	0.0927 ± 0.003

levels, such as 80% RH, we are limited to lower temperatures (37ºC) due to dewpoint constraints. At 45ºC we were limited to 60% RH, and at 52ºC it was very difficult to exceed 35% RH. In any event, we observed changes in perspiration output as a result of temperature and humidity variation. For example, increasing the humidity from 30% RH to 60% RH at 37ºC results in an increase in perspiration activity. Increasing humidity results in two principal outcomes. First, the efficiency of evaporative cooling decreases since high levels of humidity in the air permits less evaporation of sweat on the surface. As a result, sweat remaining on the surface increases in temperature and acts as an insulator to the external environment, thereby making it more difficult for body temperature regulation. Second, an increase in humidity, while keeping the temperature constant, results in an increase in the heat index, which is a parameter designed to predict the effective temperature as perceived by humans. At both temperatures, we observe an increase in axillae perspiration when the humidity is increased from 30% RH to 60% RH and 80% RH. When the humidity is held constant at 30% RH and the temperature is increased from 37ºC to 45ºC and 52ºC, we also observe an increase in axillary activity.

In the FDA monograph guidelines for antiperspirant testing, the hot room conditions are specified at ~38ºC (100ºF) and 35–40% RH. Further, subjects are allowed to acclimatize for 40 min followed by two 20-min periods of sweat collection. While the tests completed in this study do not precisely follow this protocol, our findings are very useful in illustrating the temperature and humidity effects on sudoriferous behavior. They also show the importance of dewpoint temperature as a major factor that should be considered. Dewpoint is defined as the temperature to which air must be cooled in order for water condensation to take place. The higher the RH, the more the dewpoint temperature approaches ambient temperature. When administrating clinical antiperspirant tests, one should avoid such high humidity conditions as condensation will likely occur. In our experience, we find that high dewpoint temperatures make it extremely difficult for evaporative cooling to take place. Much of the sweat remains on the skin surface, becomes hot, and does not allow new sweat to carry out cooling functions; hence the body is unable to cool itself.

A variety of other tests were also conducted and it was found that additional factors also influence the rate of sweating, such as water consumption, preconditioning climatic conditions, and exercise. Table II contains perspiration rates, again determined from the rate of perspiration between 25 and 45 min in the chamber, when other variables are introduced into the protocol. All of these clinical studies were conducted at a sauna

Table II
Perspiration Rates (g/min) at 45°C and 35% RH with the Influence of External Factors

	Subject 1		Subject 2	
	Left	Right	Left	Right
Control	0.0790 ± 0.001	0.0848 ± 0.005	0.0405 ± 0.002	0.0295 ± 0.002
Hot water	0.1020 ± 0.003	0.1019 ± 0.010	0.0639 ± 0.006	0.0562 ± 0.057
RT water	0.0829 ± 0.015	0.0799 ± 0.002	0.0464 ± 0.003	0.0321 ± 0.000
Bicycle for 15 min	0.1085 ± 0.002	0.1010 ± 0.000		
Cold acclimatization	0.0238	0.0214	0.0170	0.0140

temperature of 45°C and 35% RH. In all cases, except the cold acclimatization procedure, subjects first spent 30 min in the environmental room at 27°C and 50% RH. Drinking a glass of hot water (76°C) at $t = 20$ min in the sauna chamber resulted in a sharp increase in the firing output of the sweat glands—an increase ranging from 20% to 29% for Subject 1 in the left and right axillae, respectively, and 58% and 91% for Subject 2 in the left and right axillae, respectively. As a control, we had subjects also consume a glass of room-temperature (RT) water—measured at 22°C—also at $t = 20$ min in the sauna chamber. In this case, there appears to be a very slight increase in sweat activity, although in most cases it falls within the limits of the standard deviation. We also conducted a clinical protocol, which incorporated physical activity into the acclimatization period in the environmental room. The subject spent 15 min in the environmental room under the same conditions as in all other tests followed by a 15-min period of physical exertion on a stationary exercise bicycle (20 mph, 86 rpm, level 3). In this case, physical activity resulted in a similar increase in perspiration rate as with consumption of hot water. In the final test listed in Table II, both subjects were acclimatized in a cold room at 2°C and 80% RH for 30 min prior to immediate entry into the sauna chamber, thereby replacing the 30-min equilibration period in the environmental room at 27°C and 50% RH. As a result, the rate of perspiration decreased markedly by 70% and 75% in the left and right axillae, respectively, for Subject 1 and 58% and 53% in the left and right axillae, respectively, for Subject 2. Such experiments offer ideas for alternative equilibration techniques when testing antiperspirant actives. For example, we might be able to reduce the amount of time spent during the acclimatization phase of the study by incorporating physical activity or hot water consumption into the test protocol. Likewise, we must also consider the subject's environment prior to the clinical test. If the subject spends time in a cold environment prior to entry into the environmental room or sauna, this will certainly influence the outcome of the results. In fact, the inspiration for conducting the cold acclimatization test came from such conditions. When developing the test protocol, we noted that subjects who spent most of their day in a cold environment had much lower perspiration rates than on days when their climatic conditions were better controlled. Essentially, when subjects commented that they had a chill because their office space was unusually cool on a particular day, we observed a reduction in gravimetric output.

IR THERMAL IMAGING

IR thermography is an imaging science concerned with the measure of emitted IR radiation from objects in the electromagnetic spectrum range of 9,000–14,000 nm (9–14 μm). Thermal imaging cameras are used for a variety of different temperature-related imaging solutions including medical imaging, military applications (night vision), manufacturing situations, and research investigations. It provides a quick approach for acquiring accurate temperature measurements in the form of an image. It is a nondestructive technique that allows us to resolve the temperature distribution of objects within an image. Each image contains a two-dimensional grid (x and y), representing spatial coordinates (just like a normal digital photograph) with z information (temperature) plotted in the form of a color distribution scale. Therefore, each pixel in the image contains temperature data plotted using a distribution of various shades of colors ranging between green and white.

Figure 4 contains a series of images we obtained for one of the subjects upon entry into the environmental room, then after 30 min in the room, followed by a period of time spent in the sauna chamber. In Figure 4A, the overall surface temperature of the skin is lower than in Figures 4B–4D. This phenomenon occurs because the subject was acclimatized in an office for several hours beforehand at a lower temperature than the environmental room. After 30 min in the environmental room (Figure 4B), the surface temperature of the subject begins to increase, especially in the rostral (facial) region and the superior torso. After 10 min in the sauna (Figure 4C), peak temperature is reached at the rostral region, superior torso, and the lower limbs. The subject begins to sweat profusely after 10 min in the sauna, resulting in an overall cooling effect over all surfaces of the integument as shown in Figure 4D. Subsequent images were obtained at 30, 40, and 50 min, which showed similar behavior as that observed at 20 min. In summary, these data show that the 30-min acclimatization in the environmental room followed by the first 10 min in the sauna chamber is sufficient to bring the subject to a state of profuse sweating, which can be monitored for the last 20 min of the skin replica test. (A total time of 30 min was spent in the sauna chamber during the skin replica test.)

FLUX DENSITY MEASUREMENTS

As previously mentioned, IR imaging was used to view components of the subject's homeostatic response to rising internal temperatures, including changes in radiative dissipation and subsequent sudorific cooling. On occassion, prior to testing, the subject

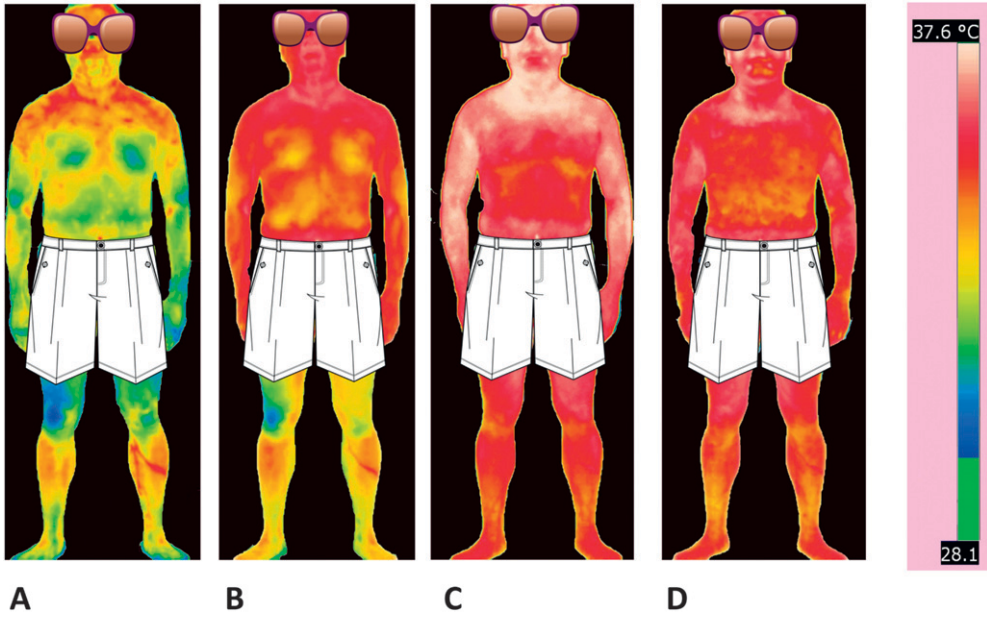

Figure 4. (A) IR images collected upon entry into the environmental room, (B) after 30 min acclimatization in the environmental room, (C) after 10 min, and (D) 20 min in the sauna. The scale for all the images is provided on the right and ranges from 28.1°C to 37.6°C. Precise measurements of temperature can be made at every pixel in the image.

mentioned that "he would not sweat much today" because he felt cold from spending much of the day in a cool working environment. Because the subject was historically known as an excellent and predictable sweater, it was hypothesized that his conditioning and subsequent sweating response may have been somewhat subdued by his recent environmental history. In addition, to minimize or to begin to appreciate the intrusion of circadian and seasonal variations on the sweating processes of a single subject within multiple studies, flux density measurements were undertaken to investigate the influence of the environmental history on the effectiveness of the final acclimatization process. Hence, an exploratory instrumental method was developed for gauging a subject's uncanny and accurate "feeling" that he/she is ready or not ready to sweat.

Closed-chamber evaporimeters (e.g., AquaFlux AF200) are devices typically used to measure TEWL, which is the steady-state flux density of water vapor diffusing through the skin barrier (17). Meaningful TEWL measurements are typically accomplished in cool and dry ambient environments to diminish the impact of ambient humidity and excessive insensible perspiration on the quality of the measurement; however, since our interests involve monitoring the physiological response to thermal stress (i.e., not TEWL), cumulative flux density profiles, as a function of time and elevated heat index, are relevant toward understanding the advent of perspiration processes (18).

For Subjects 1 and 2, flux density readings ($n = 3$) were recorded at 0, 30, and 60 min of acclimatization (30.5°C and 36.5% RH) after initial equilibration in cool (6.3°C and 66% RH), or warm (24.1°C and 28% RH) settings. At each time point, readings were taken at three different zones of the mid-volar forearm, always starting with Zone 1 and ending with Zone 3. Zone 1 was closest to the wrist, Zone 3 was closest to the elbow, and Zone 2 was sandwiched between Zones 1 and 3. Table III conveys the average number of flux density maxima ($n = 3$) visible in the flux density vs. time plots, skin surface water loss (SSWL, $n = 3$), and flux density ($n = 3$). The reported average flux density reflects the averaged steady-state flux density, or the timed-out (80 s) flux density, which are inherently larger than the subject's TEWL if influenced by insensible sweating (19). The SSWL is a combination of the quantity of water on the surface of the skin and the instrument transient, which is the water absorbed from the air during transfer of the instrument from zone to zone. Because no visible perspiration was seen, it is assumed that the number of flux maxima and the variation in the average flux readings are attributable to the pulsing influence of active eccrine glands (20,21). When a subject is equilibrated in the cool environment, a single flux maximum, which is related to the SSWL, and a steady-state flux density, which is related to TEWL, are present (e.g., 6.3°C data for Subjects 1 and 2) in the flux density vs. time plot. Exposure to warmer pre-equilibration temperatures, or to longer acclimatization times, causes a thermoregulatory response by the subject and the TEWL results are subsequently confounded by the influence of increased, steady, yet insensible, perspiration. Eventually, if the conditions warrant, eccrine activity intensifies and the number of flux density maxima within a single measurement period increases (e.g., 24.1°C pre-equilibration and 60 min acclimatization data, Figure 5 and Table III). The visible pulsing effect in the evaporimetry profile is assumed to be the summation of efflux from the asynchronous firing of several active eccrine glands within the confines of the 38.5-mm^2 measurement orifice.

For brevity, Table III summarizes only the data from the 0- and 60-min marks of final acclimatization (30.5°C and 36.5% RH), after pre-equilibration at the cool and warm conditions. Both subjects exhibited a single flux maximum, and a typical TEWL-like

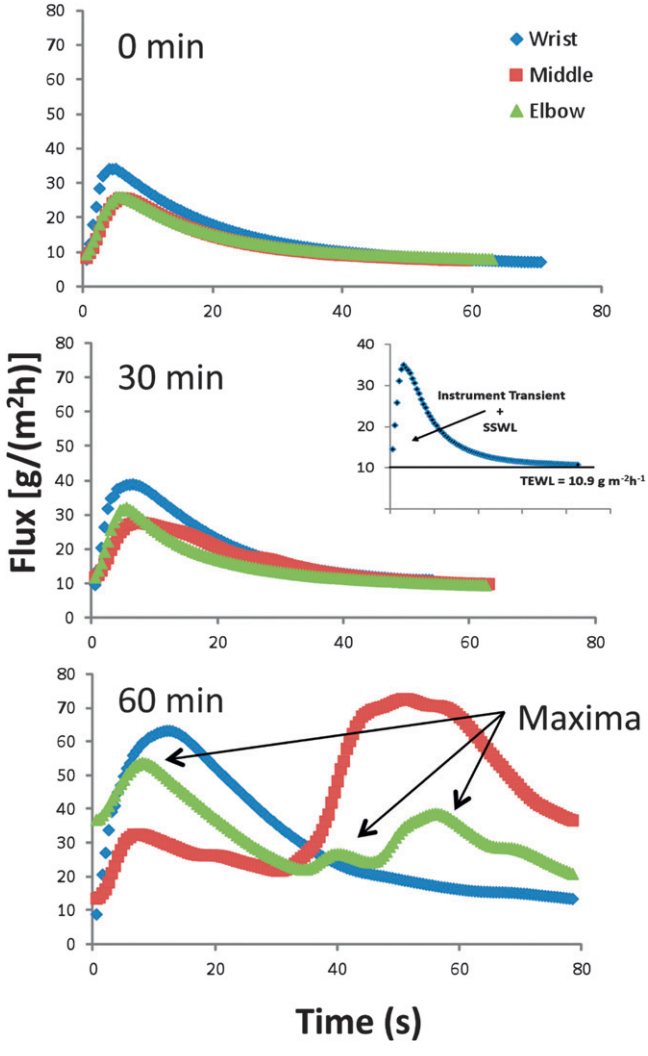

Figure 5. Average flux density vs. time profiles during acclimatization after 15 min pre-exposure to the 6.3°C environment ($n = 3$). SSWL and flux density were recorded at (A) $t = 0$ min, (B) $t = 30$ min, and (C) $t = 60$ min of acclimatization. The inset shows the determination of SSWL and TEWL from flux density vs. time profiles.

steady-state flux response at $t = 0$ of acclimatization after pre-equilibrating in the cooler environment. Further, after 30 min acclimatization, both subjects saw a rise in average flux density (+3.1–3.5 $gm^{-2}\ h^{-1}$), and the average number of flux maxima increased to 2.5 for Subject 2, yet only advanced to 1.3 for Subject 1. Similar trends are seen at the 60-min mark. The discernible increase in flux for Subject 2, which is reflected in the large reported standard deviation, was caused by a spike in the eccrine flux as the trial approached the 80 s mark (i.e., the experiment timed-out). Hence, due to sporadic sudorific activity, some of the flux density readings were not evaluated at steady state. Pre-equilibration in a warm environment introduced similar, but more exaggerated, increases in flux density. In addition, both Subjects 1 and 2 showed increases in the number of flux density

Table III
Evaporimetry Results from Acclimatization after Preconditioning Subjects in Cool (6.3°C) and Warm (24.1°C) Environments

			AVG ($n = 3$) equilibration time (30.5°C/36.5%RH)					
	AVG ($n = 3$) pre-equilibration		$t = 0$ min, $n = 3$			$t = 60$ min, $n = 3$		
Subject	15 min exposure	Key data	1	2	3	1	2	3
1	6.3°C/66% RH	AVG no. of Maxima	1.0	1.0	1.0	1.3	1.3	1.3
		SSWL (gm^{-2})	0.07 ± 0.01	0.05 ± 0.01	0.05 ± 0.01	0.09 ± 0.04	0.06 ± 0.01	0.05 ± 0.01
		Flux density ($gm^{-2}\ h^{-1}$)	14.5 ± 3.7	11.6 ± 1.7	10.7 ± 0.7	20.1 ± 2.0	15.0 ± 1.3	16.1 ± 0.8
	24.1°C 28% RH	AVG no. of maxima	2.0	1.7	1.3	3.3	2.3	2.3
		SSWL (gm^{-2})	0.15 ± 0.06	0.07 ± 0.02	0.06 ± 0.01	0.31 ± 0.25	0.11 ± 0.05	0.07 ± 0.02
		Flux Density ($gm^{-2}\ h^{-1}$)	20.6 ± 2.1	15.4 ± 1.0	16.0 ± 2.4	32.5 ± 11.6	17.5 ± 4.6	29.0 ± 20.7
2	6.3°C/66% RH	AVG no. of maxima	1.0	1.0	1.0	1.0	2.5	2.5
		SSWL (gm^{-2})	0.25 ± 0.17	0.15 ± 0.10	0.09 ± 0.02	0.33 ± 0.11	0.17 ± 0.11	0.16 ± 0.07
		Flux density ($gm^{-2}\ h^{-1}$)	10.7 ± 4.4	9.2 ± 1.4	9.0 ± 0.9	13.2 ± 1.1	25.1 ± 19.0	18.9 ± 5.5
	24.1°C 28% RH	AVG no. of maxima	1.5	1.5	1.5	4.0	2.3	2.3
		SSWL (gm^{-2})	0.27 ± 0.20	0.11 ± 0.06	0.09 ± 0.01	0.55 ± 0.11	0.27 ± 0.16	0.11 ± 0.08
		Flux density ($gm^{-2}\ h^{-1}$)	12.5 ± 1.2	13.1 ± 0.3	13.2 ± 0.2	40.0 ± 20.2	27.7 ± 23.0	29.6 ± 20

maxima—which resulted in the nonsteady-state termination of trials and contributed to higher flux density endpoints and the large, but meaningful, flux density deviations.

Figure 6 reflects the extracted steady-state flux results ($n \geq 2$, mid-volar forearm) for each subject as a function of acclimatization time. For each subject, pre-equilibration in a cool environment produced statistically unique flux density readings at the 0- and 30-min acclimatization marks ($t_4 = 3.518$ to 3.675; $p = 0.021$ to 0.024); however, the differences between the 30- and 60-min readings were not significant ($t_4 = 0.990$ to 1.071; $p = 0.345$ to 0.395). Because the 60-min readings were statistically equivalent to the 30-min flux data, the results suggest that the subjects had properly acclimated. After pre-equilibration at the warm temperature, there was an upward directional trend in the recorded flux over the 60-min acclimatization; yet, the differences were not statistically significant ($t_4 = 0.329$ to 1.212; $p = 0.292$ to 0.332) at $t = 0$, 30, and 60 min for either Subject 1 or Subject 2. Consequently, the warm pre-equilibration results suggest that the subjects were nearly equilibrated prior to entering acclimatization. When comparing the Subject 1 vs. Subject 2 cold pre-equilibration data, there was a statistical difference between the $t = 0$-min readings ($t_4 = 2.404$; $p = 0.074$). The statistical uniqueness continues at the 30-min mark ($t_4 = 2.724$; $p = 0.053$), but is only directional at the 60-min mark ($t_4 = 1.877$; $p = 0.157$). After warm pre-equilibration, there is a statistical difference in flux output at the start of acclimatization between subjects ($t_4 = 2.503$; $p = 0.067$); however, the trends are only directional at the latter measurement times ($t_4 = 1.058$ to 1.413; $p = 0.231$ to 0.400 for 30 and 60 min, respectively).

In general, the flux density results suggest that the two subjects respond differently to acclimatization after pre-equilibration in cooler conditions. Comparison of the steady-state data between subjects implies that Subject 1 has higher TEWL and, independently, perhaps a more rapid response to thermal stress than Subject 2. However, Table III suggests that although Subject 1 has a more consistent efflux of vapor, Subject 2 appears to have a higher frequency of flux pulses as proper acclimatization is approached. In practice, the latter point may correlate with trends (nonreported data) from >50 sauna study trials. Although Subject 1 unswervingly produced higher axillae sweat volumes than Subject 2 in all hot box studies, Subject 2

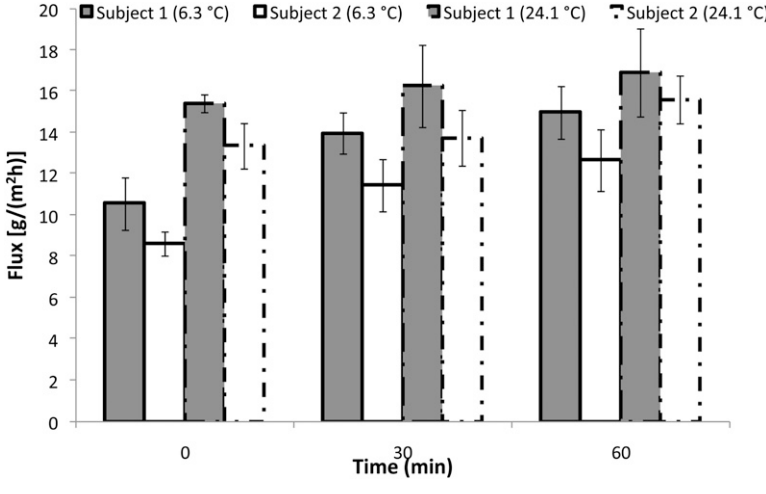

Figure 6. Steady-state flux density readings for Subjects 1 and 2 as a function pre-equilibration temperature and acclimatization time (mid-volar forearm, zone 2).

consistently perspired "sensibly" (eccrine activity) from the volar forearm earlier and more prolifically than Subject 1. Without debate, it is not statistically sound to draw solid conclusions from such a small study. However, since the two subjects were involved in >50 trials in the hot box and had become acutely familiar with their own sweating habits, trends in "I will sweat" vs. "I will not sweat" were very clearly understood prior to screening the flux density method. Hence, the authors believe that trends in flux density pulsing frequency are potentially related to "I will sweat today." Continuing, TEWL measurements are typically recorded in environments that preclude emotional and sudorific interference. In our pre-equilibration/acclimatization study, both subjects were isolated in the cool or warm conditions to curtail the inclusion of additional stresses. Initially, TEWL-like data, with TEWL-like flux density profiles, were collected after emerging from cool environments (9–14 g^{-2} h^{-1}); however, as the body warmed during acclimatization, upward trends in flux density (insensible water loss) steadily rose to plateaus. At the flux plateaus (≥30 min), both subjects clearly recognized they felt equilibrated and were "ready to sweat." Hence, although increases in insensible sweating may not correlate with imminent eccrine sweating, increases and plateauing of vapor flux may be useful in assessing the proper environmental equilibration protocol for a subject.

CONCLUDING REMARKS

We adapted an established procedure to conduct studies of antiperspirant efficacy using skin replica technology in conjunction with image analysis. Rheological analysis of skin replica gelation provided an understanding of the system's kinetic behavior allowing it to be transferred easily to the *in vivo* procedure. Gravimetric studies were carried out to determine the kinetic behavior of axillae sweating. Differences in sudoriferous behavior were found to arise depending on the environmental conditions of the test. Further, other external factors, such as diet and physical motility, were found to greatly influence sweat output in the axillae. In addition, IR thermal imaging provided insight for the overall sweating behavior with respect to the method conditions. Monitoring variations in vapor flux from the skin surface improved the understanding of proper protocols for assigning equilibration times in the test procedure. In closing, we describe an affordable hot room testing capability for antiperspirant technologies that can be established in most laboratories. Future work in this area will include a detailed analysis comparing efficacy testing of antiperspirant technologies using this technique with established FDA protocols.

ACKNOWLEDGMENTS

We would like to thank Hani Fares and Linda Foltis for their collaboration and advice on antiperspirant technology and testing protocols. Also, we greatly appreciate the encouragement and support of Bret Clark, Diane Kennedy, Ruthann Mekita, Gopi Menon, David J. Moore, Seher Ozkan, Donald Prettypaul, and Santosh Yadav. Finally, a great debt of gratitude is owed to all the volunteers involved in this study for their dedication and generous support.

REFERENCES

(1) H. J. Hurley, "The eccrine sweat glands: structure and function" in *The Biology of the Skin*, R.K. Freinkel and D.T. Woodley Eds., (The Parthenon Publishing Group, New York, 2002), pp. 47–76.

(2) M. Brandt, S. Bielfeldt, G. Springmann, and K.-P. Wilhelm, Influence of climatic conditions on antiperspirant efficacy determined at different test areas. *Skin Res. Tech.*, **14,** 213–219 (2008).
(3) K. Wilke, A. Martin, L. Terstegen, and S.S. Biel, A short history of sweat gland biology, *Int. J. Cosmet. Sci.*, **29,** 169–179 (2007).
(4) A. Martin, J. Hellhammer, T. Hero, H. Max, J. Schult, and L. Terstegen, Effective prevention of stress-induced sweating and axillary malodour formation in teenagers, *Int. J. Cosmet. Sci.*, **32,** 1–9 (2010).
(5) G. E. Folk and H.A. Semken, The evolution of sweat glands, *Int. J. Biometeorol.*, **35,** 180–186 (1991).
(6) Y. Kuno, *Human perspiration.* (Charles C. Thomas, Springfield, IL, 1956).
(7) H. H. Reller, Factors affecting axillary sweating, *J. Soc. Cosmet. Chem.*, **15**, 99–110 (1964).
(8) E. F. Adolf, *Physiology of Man in the Desert.* (Interscience Publishers, New York, 1947).
(9) M. J. Buono and N. T. Sjoholm, Effect of physical training on peripheral sweat production, *J. App. Physiol.*, **65,** 811–814 (1988).
(10) R. K. Anderson and W. L. Kenney, Effect of age on heat-activated sweat gland density and flow during exercise in dry heat, *J. Appl. Physiol.*, **63,** 1089–1094 (1987).
(11) A. Dufour and V. Candas, Ageing and thermal responses during passive heat exposure: sweating and sensory aspects, *Eur. J. Appl. Physiol.*, **100**, 19–26 (2007).
(12) J. Burry, H. F. Coulson, and G. Roberts, Circadian rhythms in axillary skin surface pH, *Int. J. Cosmet. Sci.*, **23,** 207–210 (2001).
(13) R. Keyhani, S. Scheede, I. Thielecke, H. Wenck, R. Schmucker, V. Schreiner, J. Ennen, and A. Herpens, Qualification of a precise and easy-to-handle sweat casting imprint method for the prediction and quantification of antiperspirant efficacy, *Int. J. Cosmet. Sci.*, **31**, 183–192 (2009).
(14) H. Lobo and J. Bonilla, *Handbook of Plastics Analysis.* (CRC Press, Boca Raton, FL, 2003).
(15) Department of Health and Human Services, Food and Drug Administration. Antiperspirant drug products for over-the-counter human use; final monograph. Final rule. Fed. Regist., **68,** 34273–34293 (2003).
(16) K. P. Menard, *Dynamic Mechanical Analysis: A Practical Introduction.* (CRC Press, New York, 1999).
(17) R. E. Imhoff, M. E. De Jesus, P. Xiao, L. I. Ciortea, and E. P. Berg, Closed-chamber transepidermal water loss measurement: microclimate, calibration and performance, *Int. J. Cosmet. Sci.*, **31,** 97–118 (2009).
(18) A. Takahashi, "Role of sweating on impaired skin barrier functions in atopic dermatitis," *World Allergy Congress* (2011).
(19) R.E. Imhoff, "In-vivo and in-vitro applications of closed-chamber TEWL measurements," Intensive Course in Dermato-cosmetic Sciences, 2007.
(20) M. Shibasaki, I. Yoshimitsu, and M. Kondo, Mechanisms of underdeveloped sweating responses in prepubertal boys, *Eur. J. Appl. Physiol.*, **76,** 340–345 (1997).
(21) T. Kamei, T. Tsuda, S. Kitagawa, K. Naitoh, K. Nakashima, and T. Ohhashi, Physical stimuli and emotional stress-induced sweat secretions in the human palm and forehead, *Anal. Chim. Acta*, **365,** 319–326 (1998).